Microwave Imaging of Subsurface Defects in Coated Metallic Structures Using Small Ring Resonators

Abdulbaset M. ALI and Omar M. RAMAHI
Electrical and Computer Department, University of Waterloo; Waterloo, ON, Canada
Phone: 001 519 888 4567, Fax: 001 519 746 3077; a72ali@uwaterloo.ca; oramahi@uwaterloo.ca

Abstract
Microwave testing has the advantage of detecting surface and sub-surface flaws and anomalies under coatings, paint or dirt. Thus, major application of microwave sensors is imaging to determine the shape, size, and location of buried flaws using scattered field measurements. A typical microwave system consists of transmitting and receiving antennas and requires that both sides of the material under test to be accessible. Therefore, one-sided sensors are desirable in certain applications. Electrically small ring resonators etched on printed circuit boards are good candidates as they can provide the benefit of one-sided small footprint sensors that operate at low frequencies with high lateral resolution. This work investigates a simulation study that validates the use of these resonators for imaging subsurface flaws in coated metallic structures in the S band. The results are promising.

Keywords: Microwave, imaging, metallic structures, resonators, flaws, defects, subsurface.

1. Introduction

Surface and sub-surface flaws and anomalies under coatings, paint, or dirt are increasingly being detected using microwave sensors [1]-[3]. Currently, the scattered field measurements used in determining the shape, size, and location of buried flaws [4]. Various microwave imaging modalities have been reported, as in [4]. A typical microwave testing system consists of transmitting and receiving antennas as in shown in Figure 1. Such a configuration is practical if both sides of the material under test (MUT) are accessible [4]. Hence, using open-ended waveguide sensors for imaging has the advantage of simple operation, as they are one-sided and so do not require access to both sides of the MUT [1-2]. However, to achieve the benefits low cost by operating at low frequencies, one needs to use large waveguide dimensions, leading to a large sensor footprint. Consequently, flaws will appear to be enlarged in the reconstructed image or, more specifically, the imaging will suffer from low lateral resolution [3, 5]. Additionally, open-ended waveguides can provide information about only the reflection coefficient (S_{11}). Therefore, one-sided sensors with a small footprint that provide both reflection and transmission coefficients are desirable. Electrically small near-field ring resonators etched on printed circuit boards (PCBs) are good applicants as they can provide the benefit of small footprint sensors that operate at low frequencies with high lateral resolution.

This work presents a simulation study using an ANSYS®- (HFSS™) High Frequency Structural Simulator that validates the use of electrically small near-field ring resonators for microwave imaging. In it, two models with subsurface flaws in coated metallic structures have been imaged using electrically small near-field ring resonators operating in the S band [2- 4 GHz].

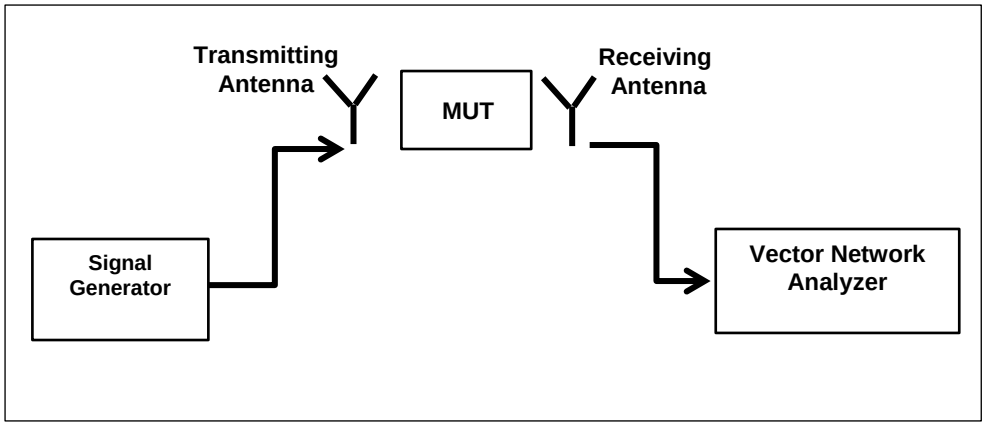

Figure 1 Typical Microwave Testing System Configuration.

2. Sensor design and operation

The sensor design is based on a microstrip transmission line with a complementary split-ring resonator (CSRR) etched in the ground plane of the PCB in use. The CSRR sensor acts as an electrically small resonator whose dimensions are smaller than the operating wavelength. Figure 2 shows the sensor's layout, where the red line is the transmission line on top of a substrate, and the green region is the ground plane on the bottom of the PCB. The sensing region is comprised of two co-centered split square rings, which form an inductor-capacitor (L-C) structure that resonated at a certain frequency. The sensor's resonance frequency can be perturbed by changing the surrounding environment of the L-C circuit (the sensing element) [6]. For example, when the sensor scans a painted or coated metallic plate, it resonates at a certain frequency (3.8 GHz). However, when it encounters a corroded region, then its resonance frequency shifts. More precisely, the transmission coefficient ($|S_{21}|$) experiences a frequency and an amplitude change (Figure3).

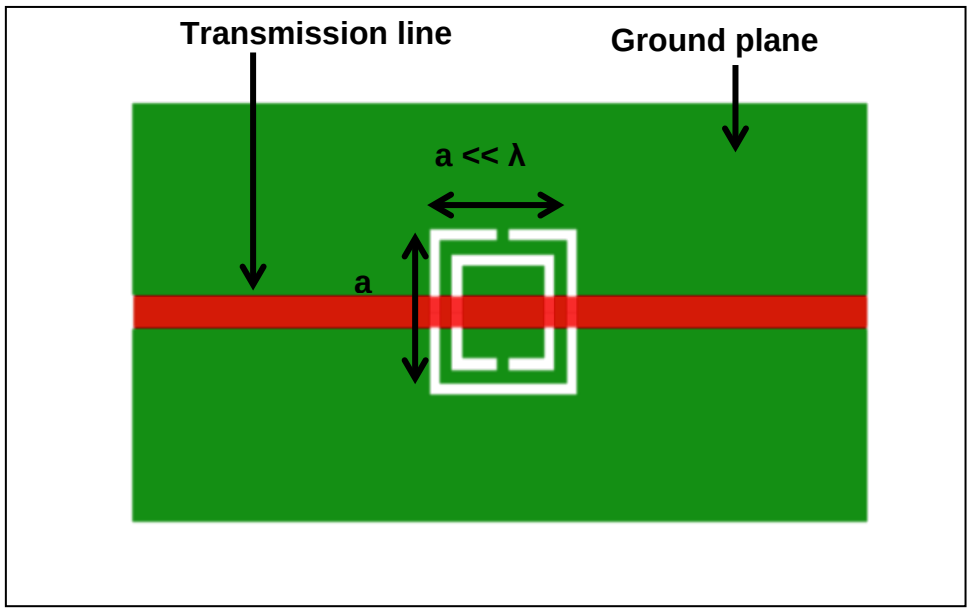

Figure 2. Used Sensor Layout

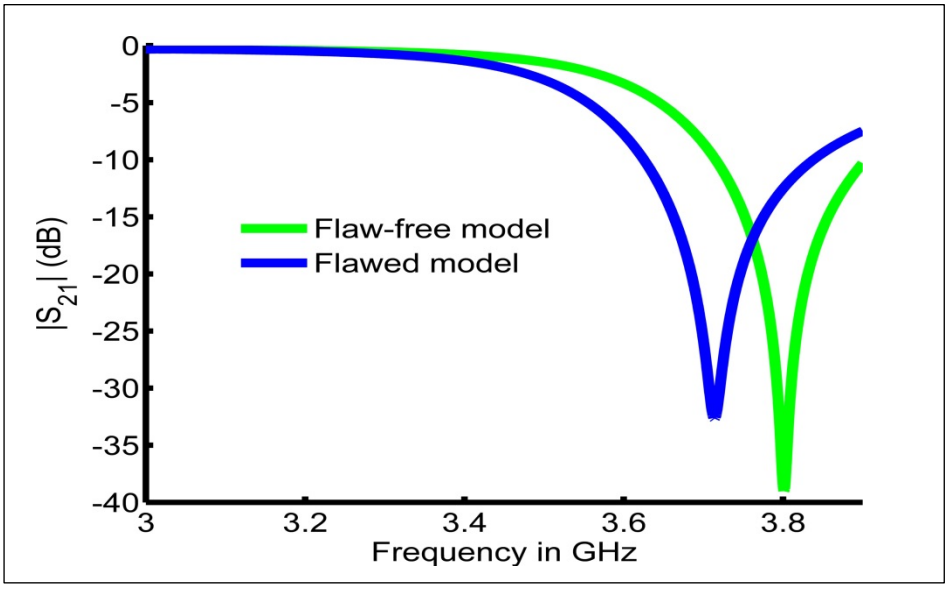

Figure 3. Transmission Coefficient Magnitude in (dB) vs Operating Frequency.

Two models of Teflon-coated Aluminum plates were simulated. The first model had only one corroded region, whereas the second had two corroded regions, with different depths. A raster scan around the flawed regions, as shown in Figure 4, was used to image the MUTs. The $|S_{21}|$ results were later transferred to a Matlab environment for post-processing.

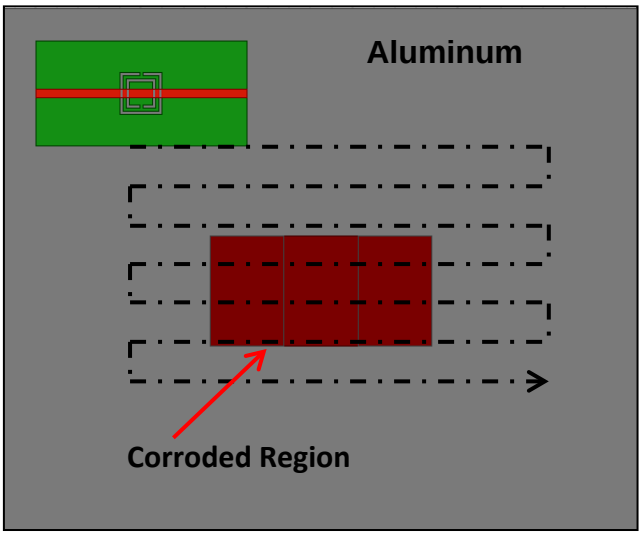

Figure 4 Raster Scan around Corroded Region in Aluminum Plate

3. Study setup and results

The first simulated MUT was an Aluminum plate of 4cm X 4cm, with a corroded region of 15mm X 7.5mm and depth of 2 mm, under a Teflon sheet of 50µm. The sensor scanned the MUT, from a stand-off distance of 0.5mm, covering an area of 2.3cm by 2.3cm (around the defect), moving with a 1mm step in a raster scan pattern to construct an image of 529 pixels. The sensor operated over a frequency range of 2–4 GHz. The sharpest images for the MUT were obtained near the top of this range (at 3.8 GHz), that is, within the sensor's resonance

frequency, while facing the flaw. The results of the scattering matrix were transformed to Matlab for post-processing. A scaled version of the reconstructed image at 3.71 GHz for the first simulation setup is shown in Figure 5. The blue rectangular region in the figure clearly shows the flawed region, and the yellow and red backgrounds correspond to the rest of the scanned area. Comparing the flaw's dimensions in the image to its real dimensions (the dashed rectangle) confirms that the reconstructed image not only detects the flaw but also characterizes it well in terms of shape and size. A second demonstration of the results is given as a surface plot (Figure 6), which is more suitable to illustrate the defect position and depth. This figure represents |S21| in dB of each 1mm x 1mm of the scanned area, where |S21| sharply declines at the corroded region (the blue part of the surface plot).

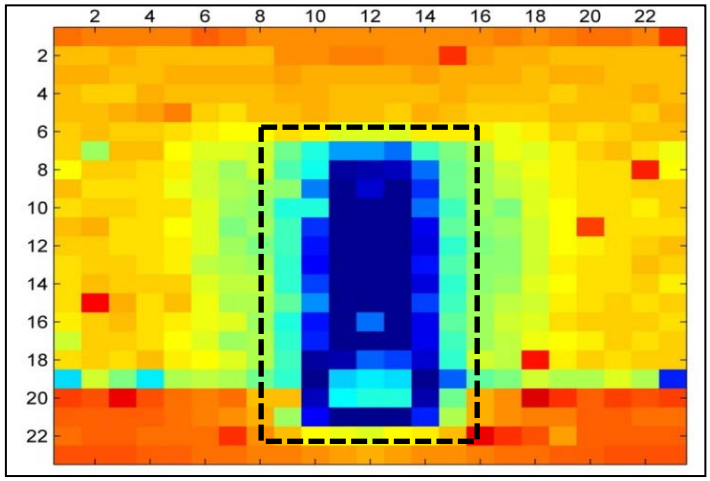

Figure 5 Scaled Image of Aluminum Plate with One Corroded Region

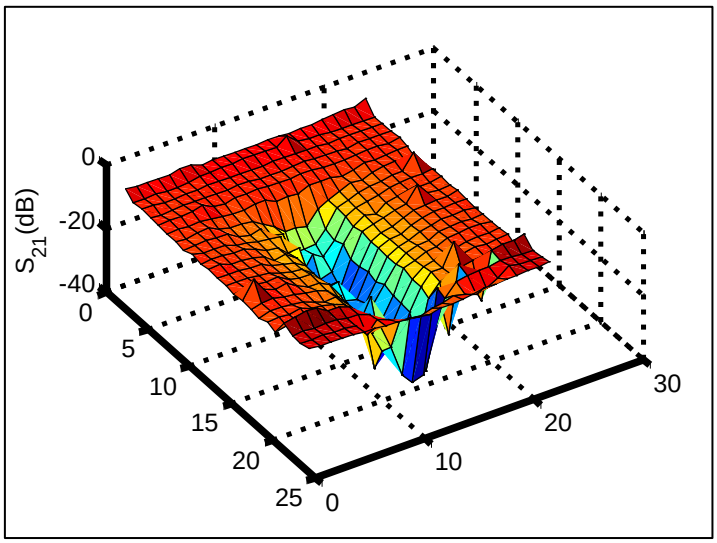

Figure 6 Surface Plot of Transmission Coefficient (S21) vs Scanned Area

The feasibility of flaw depth characterization is considered here. A Teflon-coated Aluminum plate with two corroded regions was used. The first flaw/defect (left side) was a corroded region 10mm x 7 mm, with a 2mm depth and the second flaw was 10mm x 7 mm, with a 1mm depth. The sensor scanned the MUT from a stand-off distance of 0.5mm, with a 1mm step in a raster scan pattern, constructing an image of 609 pixels for a scanned region was

2.9cm x 2.1cm. A scaled version of the reconstructed image for the second simulation setup is shown in Figure 7. The image clearly shows both flaw regions (blue rectangular regions). The region with a deeper flaw is a darker blue than the other region. The separation distance between the flawed regions is depicted clearly in the figure.

The results are illustrated as a surface plot in Figure 8, where the difference between defect depths is more clearly represented than in Figure 7. In fact, Figure 8 gives the transmission coefficient as its third dimension. The transmission coefficient magnitude difference between the flawed regions is (-5 dB). Thus, the 2mm-deep corroded region shows a deeper dip in the plot than the 1mm-deep region.

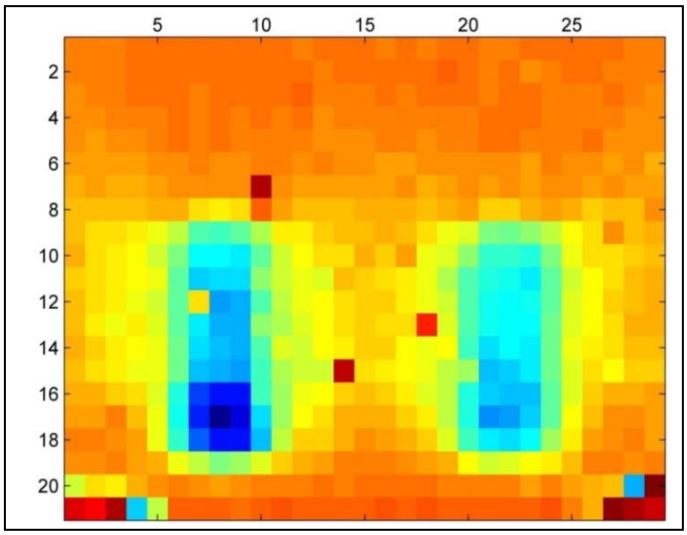

Figure 7 Scaled Image of Aluminum Plate with Two Corroded Regions

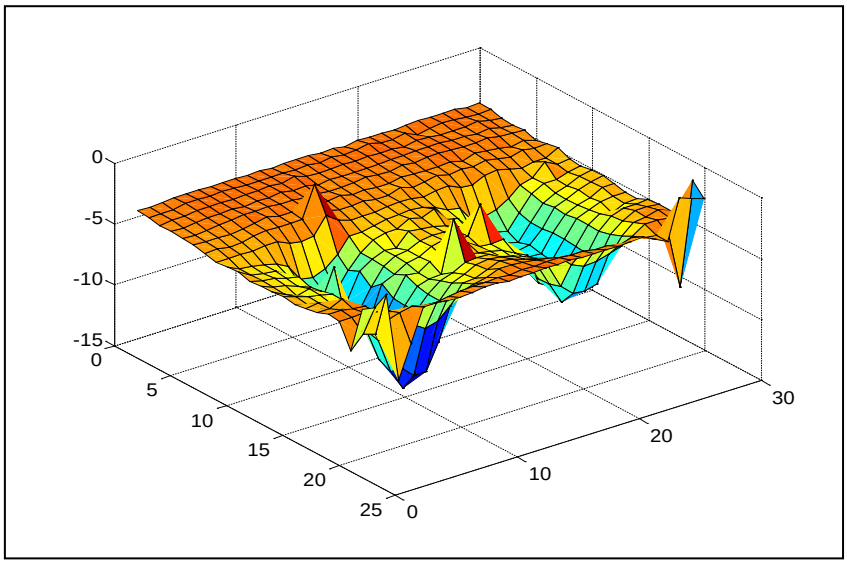

Figure 8 Surface Plot of Transmission Coefficient (S21) vs Scanned Area
for MUT with Two Corroded Regions

The results presented in Figures 7 and 8 can be further processed using curve fitting techniques or intelligent regression models to map the reflection coefficient magnitude to the physical depth of the flaw.

4. Conclusion and future work

This work has demonstrated the ability of small microwave ring resonators to image flaws in coated metallic structures. The results show sharp flaw images for corroded regions in Aluminum plates. In addition, good flaw localization and depth characterization were achieved by mapping the results to a surface plot. Future work will attempt to correlate the sensor's response to the physical flaw depths using curve fitting or regression models. Performing experimental measurements of the simulated models will be another phase of the future work.

Acknowledgements

This work was funded in part by the Libyan Ministry of Higher Education and Scientific Research and the Natural Sciences and Engineering Research Council of Canada- NSERC.

References

1. S. Kharkovsky and R. Zoughi, "Microwave and millimeter wave non-destructive testing and evaluation - Overview and recent advances," IEEE Instrumentation and Measurement Magazine, vol. 10, pp. 26–38, 2007.

2. Testing and Applied Microwave Non-destructive lab, "Microwave and Millimeter Wave NDT & E Principles, Methods and Applications," [Online]. Available: http://amntl.mst.edu/media/research/amntl/documents/Microwave_Milimeter_Wave_NDT_E_Tutorial.pdf.

3. Qaddoumi, N.N.; Saleh, W.M.; Abou-Khousa, M., "Innovative Near-Field Microwave Non-destructive Testing of Corroded Metallic Structures Utilizing Open-Ended Rectangular Waveguide Probes," Instrumentation and Measurement, IEEE Transactions on , vol.56, no.5, pp.1961,1966, 2007

4. Deng, Yiming, and Xin Liu. "Electromagnetic Imaging Methods for Non-destructive Evaluation Applications." Sensors ,Basel, Switzerland 11.12, 2011.

5. Hong Zhang, Bin Gao, Gui Yun Tian, Wai Lok Woo, Libing Bai, "Metal defects sizing and detection under thick coating using microwave NDT," NDT & E International, Volume 60, pp 52-61, 2013.

6. Boybay, M.S.; Ramahi, O.M., "Non-Destructive Thickness Measurement Using Quasi-Static Resonators," Microwave and Wireless Components Letters, IEEE , vol.23, no.4, pp.217,219, 2013